# Wannier-Stark localization of $X$ and $\Gamma$ states in GaAs-AlAs short-period superlattices

D. M. Whittaker, M. S. Skolnick, G. W. Smith, and C. R. Whitehouse
*Royal Signals and Radar Establishment, St. Andrews Road, Malvern, Worcestershire WR14 3PS, United Kingdom*
(Received 26 February 1990)

We report the observation of Wannier-Stark localization effects for both $X$- and $\Gamma$-derived miniband states in GaAs-AlAs superlattices in an axial electric field. The splitting of the optical interband transitions into Stark ladders is observed in both photoconductivity and photoluminescence. The behavior of the light-mass $\Gamma$ states is interpreted with use of a new theoretical model for the superlattice exciton states in an axial electric field. We show that for the small $\Gamma$-$X$ separations in the structures considered it is necessary to include the effects of $\Gamma$-$X$ mixing in order to understand the behavior of the $X$ states.

## I. INTRODUCTION

There have been a number of reports recently of the observation of Stark-ladder behavior in the optical transitions of type-I superlattices (SL's).[1-5] Wannier-Stark localization occurs when an axial electric field breaks the SL miniband down into a series of localized states, peaked in sequential wells and separated in energy by approximately the change in electrostatic energy over a single period.[6] The effect can be detected optically by observing transitions between holes and electrons peaked in separate wells, giving a ladder of roughly equally spaced peaks, which are labeled according to the electron-hole separation, in periods, as indicated schematically in Fig. 1. The strength of the peaks falls rapidly with separation as the overlap between the electron and hole wave functions decreases. In a type-I SL under applied electric field, both electrons and holes are localized predominantly in the same, narrower-band-gap, "quantum-well" regions of the structure, and so the separations are integer numbers of periods [Fig. 1(a)]. Stark-ladder behavior can also be observed in type-II SL's, for which the transitions are slightly different, since the electrons and holes are confined in adjacent regions of the structure. The Stark-ladder peaks thus correspond to separations of $\frac{1}{2}, \frac{3}{2}, \ldots$ periods,[6] as indicated in Fig. 1(b). Such a type-II band configuration occurs for the $X$-electron–$\Gamma$-hole transitions in a GaAs-AlAs superlattice,[7] for which the holes are confined in the GaAs and the electrons in the AlAs. Optical transitions involving such states are thus "indirect" in both real and **k** space.

In this paper, we present the first observations of $+\frac{1}{2}$ and $-\frac{1}{2}$ Stark-ladder transitions in both photoconductivity (PC) and photoluminescence (PL) spectra from (11,8) and (10,8) monolayer (ML) (GaAs, AlAs) type-II SL's. Meynadier *et al.*[8] have previously reported $+\frac{1}{2}$ transitions in the PL spectra of a GaAs-AlAs SL, but the $-\frac{1}{2}$ transition was not observed. In our SL's, the $X$ and $\Gamma$ electron states are close to crossover, with the bottom of the $\Gamma$ miniband approximately 30 and 50 meV higher in energy than the $X$ states for the (11,8) and (10,8) structures, respectively. The 0 and $\pm 1$ transitions for the $\Gamma$ states are observed in the PC spectra, and their type-I behavior is contrasted with that observed for the $X$ states. A study of $X$ and $\Gamma$-related transitions in the present structures using electroreflectance spectroscopy is described in a separate publication.[9]

Previous theoretical treatments of the Stark ladder have been based upon the single-particle behavior in an electric field.[5] This successfully predicts the breakdown of the SL miniband in the field, but cannot be correct in detail since it neglects the excitonic contributions arising from the Coulomb interaction between the electron and hole. Recently, Whittaker derived an envelope-function-type model for the SL exciton,[10] which can readily incorporate an axial electric field. In the present paper, we present such a treatment of the excitonic interaction for

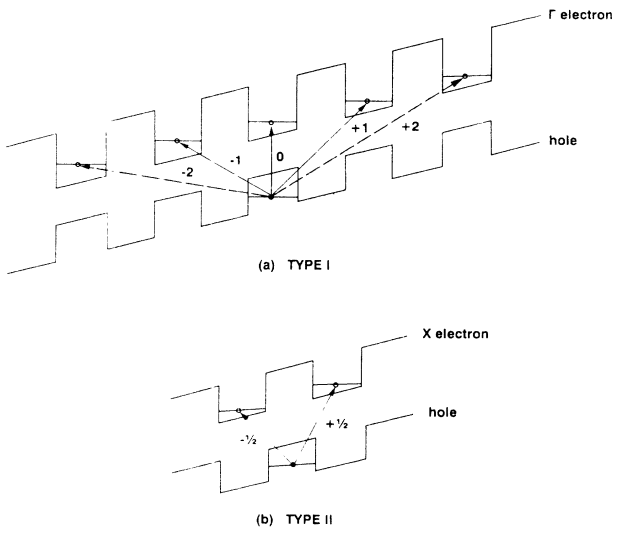


FIG. 1. Schematic diagram of band lineups for a superlattice in an electric field, showing the type-I [Fig. 1(a)] and type-II [Fig. 1(b)] Stark-ladder transitions. These correspond respectively to the $\Gamma$ and $X$ transitions in a GaAs-AlAs structure.

the (10,8) GaAs-AlAs SL and compare the theoretical predictions with the experimental results.

## II. EXPERIMENTAL DETAILS

The experiments were carried out on two nominally undoped GaAs-AlAs SL structures grown by molecular-beam epitaxy with GaAs well widths of either 11 or 10 ML (1 ML $\simeq$2.83Å) in each case separated by 8-ML AlAs barriers. The SL's consisted of 100 repeats of the (11,8) or (10,8) period[11] grown on top of a 1-$\mu$m, $n=1\times10^{18}$ cm$^{-3}$ GaAs buffer layer on an $n^+$-type GaAs substrate. The whole structure was capped by 250 Å of undoped GaAs. Electric fields were applied to $\sim$80 Å semitransparent Au Schottky-barrier contacts on mesa structures of sizes 0.5–2 mm, with Ohmic contact made to the $n^+$-type GaAs substrate. Capacitance-voltage measurements showed that the structures were depleted under the biases studied, so that all the applied voltage was dropped across the SL.

PL was excited with $\sim$1 W cm$^{-2}$ of 5145 Å radiation from an Ar-ion laser, dispersed by a 0.75 m spectrometer, and detected using a cooled GaAs photomultiplier. The light source for the PC experiments was $\sim$0.2 W cm$^{-2}$ of tunable radiation from an Ar-laser-pumped dye laser, covering the photon-energy range 1.77–1.90 eV. The PC spectra were recorded under constant-voltage conditions using a high-sensitivity current amplifier and conventional lock-in techniques. For most of the experiments, the sample temperature was either 2 or 5 K. There was no observable temperature dependence of the spectra over this range.

## III. EXPERIMENTAL RESULTS

Figure 2 shows the PC spectra for the (10,8) SL at a temperature of 4 K, at various values of applied voltage. +0.8 V bias applied to the Schottky barrier corresponds to the flatband, zero-field condition. Thus an applied bias of, for example, −0.2 V (+0.2+0.8=1.0 V total bias) gives rise to an electric field in the SL of $1.9\times10^4$ V cm$^{-1}$.

The $\Gamma$-state transitions are observed to dominate the spectra in Fig. 2, as expected, since they are direct both in real and **k** space. Nevertheless, the $X$ states are visible as weak features to lower energy with $\sim$0.15%–0.5% of the intensity of the $\Gamma$ transitions, the precise value depending on the value of the applied field. The $\Gamma_0$ peak is well resolved and can be seen to strengthen as the field is raised (see theoretical discussion in Sec. IV). Also observed are the $\Gamma_{\pm1}$ peaks, corresponding to transitions involving electrons and holes in GaAs layers separated by one period [Fig. 1(a)]. By contrast, the $X$ spectra are split into $X_{-1/2}$ and $X_{+1/2}$ peaks, corresponding to transitions involving electrons and holes in adjacent AlAs and GaAs layers [Fig. 1(b)].

Figure 3 shows the PL spectra at 2 K of the (10,8) SL at various values of applied voltage. The spectra again clearly show the splitting of the $X$ exciton into $X_{-1/2}$ and $X_{+1/2}$ states. Also apparent is the $\Gamma$ PL, which for this structure is at 40 meV higher energy than the $X$ transitions and so is very much weakened by the thermalization of the electron population. In the raw spectra at higher fields, an extra peak appears in the zero-field position. This is due to a very weak signal from regions of the structure in which there is no field, and so has been removed from the plotted spectra, as indicated by the dashed lines.

In the flatband condition, +0.8 V [Fig. 3(a)], additional peaks are observed, labeled $Y_1$, $Y_2$, and $Y_3$. These are due to momentum-conserving phonon-assisted PL transitions in the indirect-gap SL.[7,12] Under electric fields of $\sim1\times10^4$ V cm$^{-1}$ and above [Figs. 3(b)–3(e)], the phonon satellites disappear, which may indicate that the strength of the phonon coupling is enhanced by extrinsic localization effects at zero field.

As the field is increased [Figs. 3(b)–3(e)], the overall intensity of the PL falls rapidly, since nearly all the photocreated carriers are swept out of the SL before recombination occurs. This effect is particularly important for the $X$-state recombination, due to the small oscillator strength, and hence long radiative lifetime, of order 1

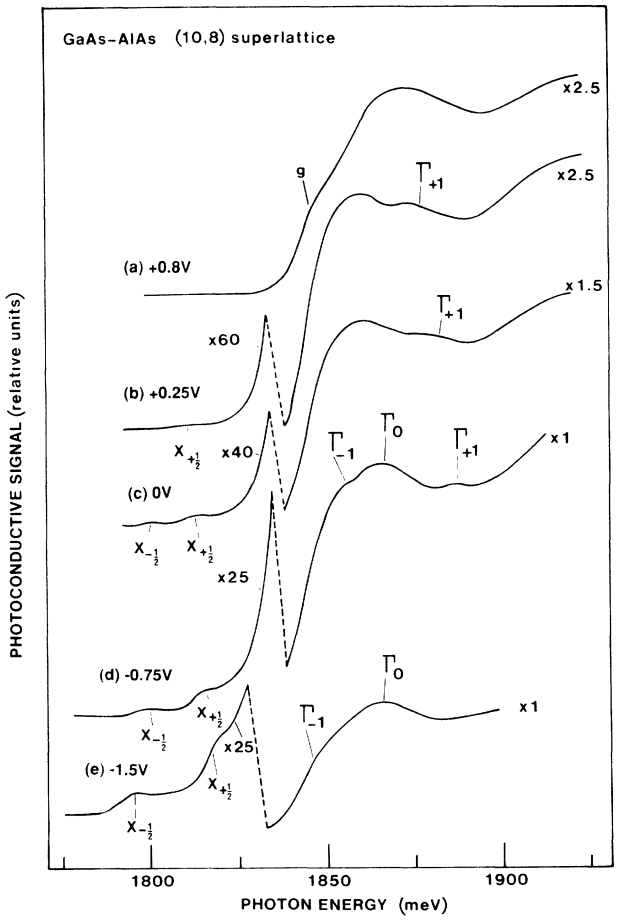


FIG. 2. Photoconductivity spectra at 4 K for the GaAs, AlAs (10,8) SL as a function of applied voltage. +0.8 V corresponds to approximately zero field in the SL. Splitting of the $\Gamma$ transitions into $\Gamma_{+1}$, $\Gamma_0$, and $\Gamma_{-1}$, and $X$ transitions into $X_{-1/2}$ and $X_{+1/2}$ is observed. The relative gain setting for each spectrum is indicated. The $\Gamma_0$ signal at high field corresponds to a photoinduced current of $\sim$10 $\mu$A.

$\mu$s,[12] associated with such transitions. By contrast, the $\Gamma$-state recombination time is $\sim 0.5$ ns, and so the $\Gamma$-derived PL is expected to be less strongly quenched by the applied field. This can be seen by comparison of Figs. 3(b) and 3(d), where the ratio of the $\Gamma$-to-$X$ PL intensities increases by a factor of $\sim 15$ between $-0.2$ and $-1.45$ V applied bias (electric field increasing from $1.9\times10^4$ to $4.3\times10^4$ V cm$^{-1}$). The ratio of the intensities of the two $X$ peaks also varies with field, the lower-energy state dominating in weak fields, the higher-energy state in strong fields. The origin of this variation is discussed in Sec. IV.

The broad shoulder which appears on the low-energy side of the exciton peaks in Figs. 3(b)–3(d) is defect related and increases in prominence with increasing electric field and temperature, both of which act to quench the excitonic PL.

The PL results for the (11,8) structure are shown in Fig. 4. They are very similar to those for the (10,8) SL, except in this case the $\Gamma$-related PL is only 18 meV higher in energy than the $X$ transitions. Once again, splitting of the $X$ PL into $X_{-1/2}$ and $X_{+1/2}$ peaks is observed, with the $-\frac{1}{2}$ transition dominating in low fields [Figs. 4(b) and 4(c)], the $+\frac{1}{2}$ at higher fields [Figs. 4(e) and 4(f)]. As for the (10,8) structure, strong quenching of the PL signal with applied bias is found. PC spectra for the (11,8) sample were also studied with $\Gamma_{-1}$, $\Gamma_0$, and $\Gamma_{+1}$ transitions, again observed at high field, but the $X$-related transitions could not be resolved because of their proximity to the dominant $\Gamma$ transitions.

Figures 5 and 6 are fan diagrams giving the positions of the spectral features as a function of applied bias for the (10,8) and (11,8) structures, respectively. Both PC and PL results are shown, with a Stokes shift of $\sim 10$ meV for the $\Gamma$ states at zero electric field.[13] The behavior is clearly very similar in the two structures. The major difference between them is that the (10,8) SL has larger

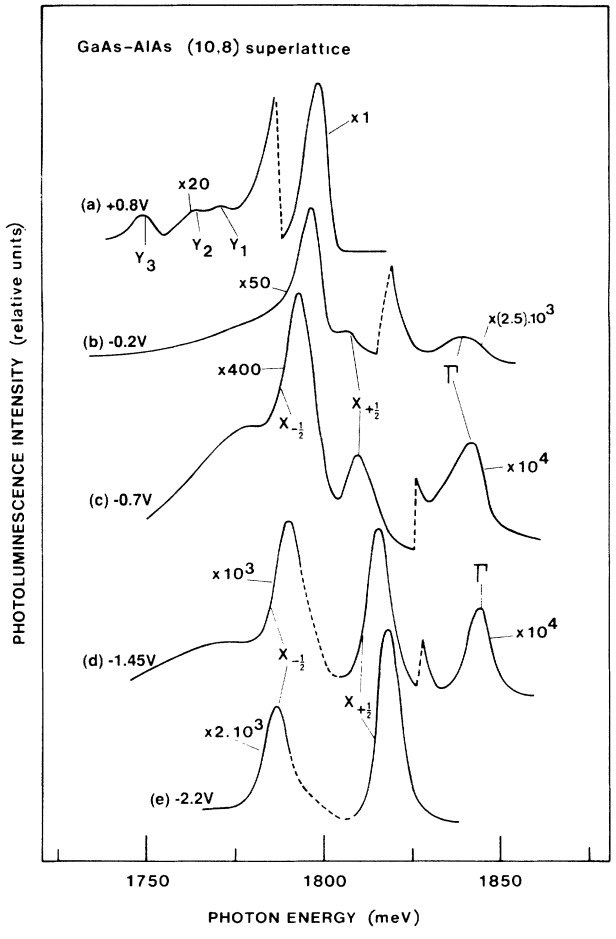


FIG. 3. Photoluminescence spectra at 2 K of the (10,8) SL for various applied voltages. Splitting of the PL in the type-II SL into $X_{-1/2}$ and $X_{+1/2}$ transitions is clearly seen. With increasing applied bias, a very strong quenching of the PL is observed, as indicated by the gains on the spectra. The dashed regions at $\sim 1800$ meV correspond to parts of the spectra obscured by signal from areas of low electric field.

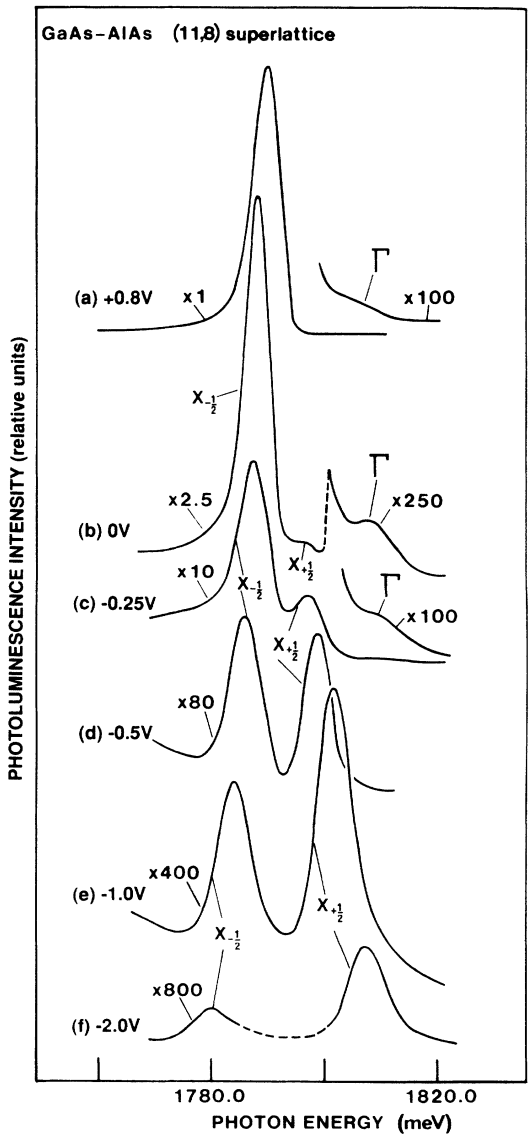


FIG. 4. As in Fig. 3, but for the (11,8) superlattice.

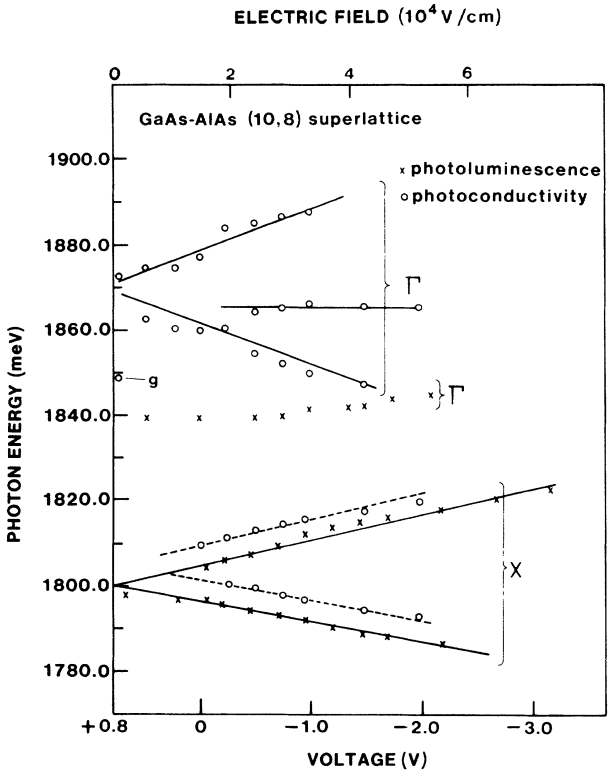


FIG. 5. Fan diagram showing the positions of the (10,8) SL spectral peaks as a function of applied voltage. The solid lines are guides to the eye, but have the correct slope for the Stark-ladder transitions in the high-field limit. Crosses represent the PL transitions, circles the PC transitions.

miniband widths and a greater $\Gamma$-$X$ separation. In both figures it is seen that the $X_{+1/2}$-$X_{-1/2}$ splitting in the high-field region is, to a very good approximation, equal to one-half of the $\Gamma_{+1}$-$\Gamma_{-1}$ splitting. This is exactly as expected since for the $X_{\pm 1/2}$ states the splitting corresponds to the potential drop across one period, whereas for the $\Gamma_{\pm 1}$ states the drop is across two periods. Furthermore, the observed shift rates and splittings correspond very closely, within $\sim 10\%$, to those expected from the known SL period, and total voltage dropped across the undoped region of the structure.

## IV. THEORETICAL TREATMENT, FITTING OF RESULTS, AND DISCUSSION

An exact treatment of the exciton problem for a SL in an electric field is complicated by the fact that there are no true eigenstates, merely resonances which can decay by Zener tunneling between minibands. However, the tunneling probability is generally small, and so it is convenient to restrict the Hamiltonian to a basis consisting of states from a single miniband.[10] This simplifies the calculation at the expense of losing the possibility of such effects as the quantum-confined Stark effect (QCSE),[14] which arise from the mixing of states from different minibands by the applied electric field. For the structures considered here, the periods are so short that the QCSE is expected to be negligible in the available range of fields.

Using such a basis, an envelope-function-type description of the exciton wave function is derived:

$$\Phi(\mathbf{r},z_e,z_h)=\Psi(n,\mathbf{r})f_e(\hat{z}_e)f_h(\hat{z}_h)\ , \tag{1}$$

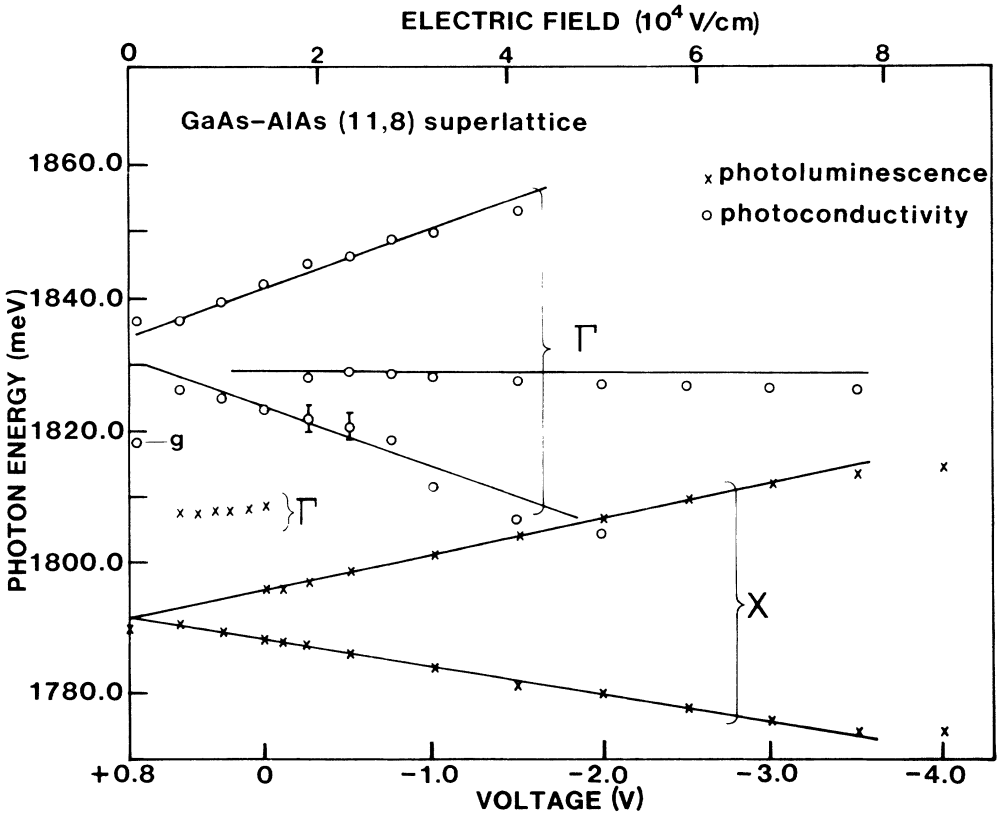


FIG. 6. As in Fig. 5, but for the (11,8) SL.

where $f_e(\hat{z}_e)$ and $f_h(\hat{z}_h)$ are the superlattice periodic wave functions, with $\hat{z}_e$ and $\hat{z}_h$ ranging only over a single period. $\Psi(n,\mathbf{r})$ is the superlattice envelope function, with $\mathbf{r}$ and $nd$ ($d$, the SL period, and $n$ integer for $\Gamma$ states and a half-integer for $X$ states) the radial and axial components of the electron-hole separation. $\Psi$ is an eigenstate of the Hamiltonian[10]

$$H=-\frac{1}{2\mu_t}\nabla_{\mathbf{r}}^2+T_l+V_n(\mathbf{r})+Fnd \ , \tag{2}$$

where $\mu_t$ is the reduced in-plane mass and $F$ the axial electric field. The axial kinetic energy operator $T_l$ can be written in terms of inter-well-hopping matrix elements, chosen by fitting to the miniband dispersion. These are dominated by the nearest-neighbor terms

$$T_l\Psi(n,\mathbf{r})=\frac{1}{2\mu_l d^2}[2\Psi(n,\mathbf{r})-\Psi(n+1,\mathbf{r})-\Psi(n-1,\mathbf{r})] \ , \tag{3}$$

where $\mu_l$ is the miniband-zone-center reduced effective mass. $\Delta n=2$ and greater terms may be added if required to provide a good fit to the miniband dispersion. $V_n(\mathbf{r})$ is an effective electron-hole interaction, related to the real Coulomb interaction $U(\mathbf{r},z)$ by

$$V_n(\mathbf{r})=\int d\hat{z}_e \int d\hat{z}_h \, U(\mathbf{r},\hat{z}_e-\hat{z}_h+nd)|f_e(\hat{z}_e)|^2\,|f_h(\hat{z}_h)|^2 \ . \tag{4}$$

For large $n$ and $r$, $V_n(\mathbf{r})\rightarrow U(\mathbf{r},nd)$, but at short range it is modified, due to the averaging over the SL period. For a bare Coulomb interaction, this leads to a logarithimic singularity as $r\rightarrow 0$ on $n=0$.

Solutions are obtained by using the two-dimensional (2D) exciton states [labeled $(n,n_r)$, where $n_r$ is the radial quantum number] in the uncoupled planes as a basis set, within which the coupling term $T_l$ is diagonalized. Since this basis can only contain a finite number of states, only the first few bound states on each plane are included. As a result, the continuum part of the spectrum is not calculated, and so exact comparisons with experimental spectra are not possible. In particular, in regions of the spectrum where the background density of states is large, there may be considerable mixing of the continuum with the calculated "bound" states, leading to a broadening of the "bound"-state peaks.

The calculation is carried out using miniband wave functions calculated from Bastard's three-band $\mathbf{k}\cdot\mathbf{p}$ theory for the light particles.[15] The electron masses are obtained from the same model, by considering the shift in energy when a small in-plane component is added to the momentum, and are close to the bulk GaAs value. In-plane heavy-hole masses of $\sim 0.18m_0$ are used, as calculated from the two-band Luttinger model of Altarelli, Ekenberg, and Fasolino.[16]

Figure 7 shows the calculated peak positions as a function of the applied electric field for the (10,8) structure; the area of the plotted circle is proportional to the spectral intensity of the peak. In the plot, a cutoff in intensity has been imposed. Peaks weaker than 5% of the intensity of the strongest peak are not included. The experimental points are plotted on the figure as crosses; an arbitrary shift in energy has been applied in order to line up the strongest $n=0$ theoretical and experimental peaks at high field.

The behavior of the solutions is fairly straightforward at high fields. The effect of the field is to break down the superlattice miniband, uncoupling the individual wells. Thus the eigenstates are similar to the basis states and can be well, though not exactly, described by the same quantum numbers $(n,n_r)$. The strongest peak is the (0,0) state, which is located at an energy equal to the miniband center minus the 2D exciton binding energy of the $n=0$ basis state. There are also distinct peaks for all $(n,0)$ states, arranged at the appropriate binding energy below an energy $Fnd$ from the center of the miniband. These states get their oscillator strength from the probability of being at $n=0$, which falls off rapidly with $n$ and with increasing field. For a given $n$, the $-|n|$ state will always be stronger than the $+|n|$ state. The reason for this can be seen from a simple perturbation argument: The greater binding energy of the (0,0) state means it is always closer in energy to the $-|n|$ state, which therefore mixes more strongly with it than the $+|n|$ state and thus has the greater oscillator strength. The experimental peaks are not well enough resolved to make accurate comparisons of the line strengths, but the expected asymmetry is apparent in both the oscillator strengths [Fig. 2(d)] and energies (Figs. 5–7) of the $\Gamma_{\pm 1}$ transitions.

At lower fields, the interpretation of the spectra becomes much more complicated. When the separation $Fd$ is of the same order as the miniband width, the coupling term becomes more important, and the basis states mix strongly, with anticrossing becoming very apparent. As the field is reduced, the first anticrossing occurs when the strongest $n=0$ state is approached by $n=-1$ states; so it moves up in energy, and its oscillator strength is transferred to the lower-energy states (Fig. 7). This behavior can be seen in the experimental results: For the (10,8) SL, the oscillator-strength transfer occurs between $-0.75$ and 0 V applied bias [Figs. 2(d) and 2(c)], while the high-field-energy variation of the $n=0$ peak in the (11,8) structure is apparent in Fig. 6, between $-2.5$ and $-1$ V. As a result of the mixing, an appropriate description of the states is difficult to find. The strongest state always has a wave function dominated by the (0,0) basis state, but as the field is reduced, it passes through all the $n<0$ states to become the ground-state exciton peak at zero field. Hence the theoretical spectra are very complicated at low field, with many peaks of similar intensity, though this behavior is not resolvable in the experimental results. By zero applied field, these peaks have combined to produce the SL exciton, 7 meV below the miniband edge, and a broad resonance, the saddle-point exciton, within the miniband.[3,17,18] Because of the restricted size of the basis set used, the saddle-point exciton is not well reproduced in the present calculation.

By comparison with the theoretical treatment, we identify the shoulder at 1847 meV, labeled $g$ [Figs. 2(a) and 5], as arising from the ground-state exciton derived from the bottom of the SL miniband under flatband conditions. A

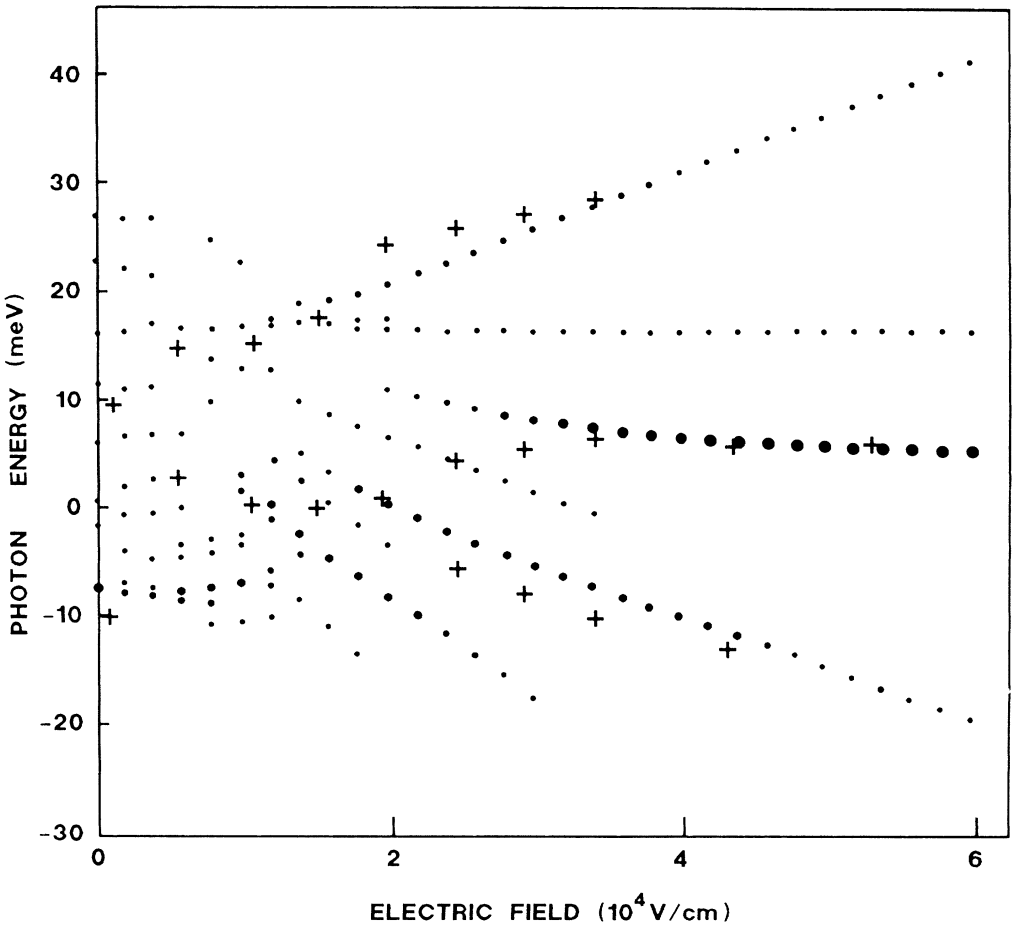


FIG. 7. Theoretical fan diagram for Γ-derived exciton peaks in the (10,8) SL. The zero of energy is the bottom of the miniband. Theoretical points are plotted as circles, with area proportional to the intensity of the peak. Experimental points are shown as crosses. The figure clearly shows the transfer of oscillator strength from the $\Gamma_0$ peak at high field to the exciton state below the bottom of the superlattice miniband at zero field.

similar feature is observed for the (11,8) structure (Fig. 6). The very broad peak at ~1870 meV in Fig. 2(a) arises from the saddle-point-exciton resonance. The blue shift of the exciton peak between zero and high field is half the miniband width, minus the difference between the exciton binding energies in the two limits (~5 meV here). We thus deduce experimentally that the miniband widths of the (10,8) and (11,8) SL's are 40 and 30 (±5) meV, respectively, in good agreement with the theoretical values of 37 and 31 meV obtained from three-band $\mathbf{k}\cdot\mathbf{p}$ theory.

The above theory can also be applied to the $X$ states. These are expected to be $X_z$ derived, due to the anisotropy of the $X$ mass,[19] as is confirmed by the weak-momentum-conserving phonon satellites observed in the PL spectra.[19] The combined miniband width for the $X$ states is small, just a fraction of a meV due to the large $X_z$ mass, $\sim m_0$, along the growth axis; so the interwell coupling is weak, and only the $n=\pm\frac{1}{2}$ states need be considered. From symmetry, provided there is no QCSE, the uncoupled exciton states in these two layers will be identical, and so mixing will only occur between equivalent eigenstates. The two-state mixing problem is easily solved. At zero field, there are symmetric and antisymmetric solutions, separated in energy by the miniband width; all the oscillator strength is in the lower, symmetric state. As the field is applied, the symmetry is broken, and so the higher energy state gains strength. In the "high-field" regime, which is actually reached at very small fields for the $X$ states, when the electrostatic energy is greater than the miniband width, there are simply two superimposed 2D excitonic spectra, with equal oscillator strengths, separated in energy by $Fd$.

This is clearly not the case in the experimental PL results, for which the $X_{+1/2}$ state steadily increases in intensity relative to the $X_{-1/2}$. Such a trend is expected as a result of the QCSE at sufficiently high fields,[8] but because of the short periods of our SL's, the difference in intensities is predicted to be no more than a few percent at the fields we have considered. However, it must be remembered that the transition is indirect in $\mathbf{k}$ space and so only gains spectral strength through mixing with Γ-like components, which will differ for the two $X$ states due to their different separations from the Γ states. It is not established whether the mixing is dominated by the potential discontinuity at the heterointerface or by disorder, but analysis of the variation of radiative recombina-

tion rate with hydrostatic pressure, and hence $\Gamma$-$X$ separation, leads to a value of the mixing matrix element of $\sim 2$ meV in a very similar (12,8) structure.[12] Since this value is small compared with the $\Gamma$-$X$ separations considered here, first-order perturbation theory can be applied to give a predicted intensity ratio of

$$\frac{I(X_{+1/2})}{I(X_{-1/2})} = \left[ \frac{E_{\Gamma_0} - E_{X_{-1/2}}}{E_{\Gamma_0} - E_{X_{+1/2}}} \right]^2 . \quad (5)$$

Application of this formula provides a qualitatively correct description of the experimental results in the high-field region. Taking, for example, the (10,8) structure at $-2.2$ V applied bias ($5.6 \times 10^4$ V cm$^{-1}$), the experimental $I(X_{+1/2})/I(X_{-1/2})$ ratio is 1.9, whereas Eq. (5) predicts a value of 2.8, in reasonable agreement with experiment. The perturbation result also explains why the $I(X_{+1/2})/I(X_{-1/2})$ ratio is greater for the (11,8) structure than the (10,8) [compare Figs. 3(c), 3(d), and 4(e)] at a given electric field, since the $\Gamma_0 - X_{+1/2}$ separation is smaller for the (11,8) SL. However, Eq. (5) tends to overestimate the ratio: In particular, for small fields it predicts an $I(X_{+1/2})/I(X_{-1/2})$ ratio tending towards unity, while the experimental values approach zero. The most likely explanation is that, since we are considering a luminescence process, prior to the transition there is significant relaxation of carriers from the higher-energy $X_{+1/2}$ exciton state into the $X_{-1/2}$ state.[20] This hypothesis is supported by measurements at higher temperatures for the (10,8) structure at a bias of $-0.5$ V: The ratio of the $X_{+1/2}$ to the $X_{-1/2}$ intensities is found to increase from a value of 0.16 at 4 K to close to unity at 30 K. Comparison with the PC spectra, which are not affected by thermalization, also supports the model. For example, the $X_{+1/2}$ and $X_{-1/2}$ PC transitions in Fig. 2(d) ($-0.75$ V) are of very similar strengths, whereas in PL [Fig. 3(c) at $-0.7$ V] the $X_{-1/2}$ transition is $\sim 3$ times stronger.

It is difficult to make any more precise statements about the effects of thermalization on the $I(X_{+1/2})/I(X_{-1/2})$ ratio in PL than those presented above, since the dynamics of the relaxation between the two states are determined by a competition between radiative and nonradiative recombination, and the scattering process, presumably phonon assisted, between them. However, it is clear that at low fields, the nonradiative processes are less important than at high fields, as can be seen by the rapid reduction in the absolute PL intensity with field. Thus the exciton lifetime must decrease quickly with field, leading to a considerable reduction in the time over which relaxation may occur; so the thermalization process is expected to be more complete at low field than at high field. This is in accord with the experimental observations, which show that the $I(X_{+1/2})/I(X_{-1/2})$ ratio tends to zero at low fields due to thermalization, whereas at high field the ratio is reasonably well described by Eq. (5).

## V. CONCLUSIONS

The effects of an applied electric field on GaAs-AlAs short-period superlattices, with $\Gamma$ and $X$ states close together in energy, have been described. Stark-ladder phenomena have been observed for both $\Gamma$ and $X$ miniband states in photoconductivity and photoluminescence spectra. A theoretical treatment of exciton states in a superlattice under applied electric field has been shown to provide a good semiquantitative description of the results for the $\Gamma$ states. It has also been demonstrated that the effects of $\Gamma$-$X$ mixing and thermalization processes must be taken into account in order to understand the behavior of the intensities of the electric field split $X$ states in photoluminescence.

## ACKNOWLEDGMENTS

We thank P. C. Klipstein for helpful comments on the manuscript.

[1] E. E. Mendez, F. Agullo-Rueda, and J. M. Hong, Phys. Rev. Lett. **60**, 2426 (1988).

[2] P. Voisin, J. Bleuse, C. Bouche, S. Gaillard, C. Alibert, and A. Regreny, Phys. Rev. Lett. **61**, 1639 (1988).

[3] J. Bleuse, P. Voisin, M. Allovon, and M. Quillec, Appl. Phys. Lett. **53**, 2632 (1988).

[4] F. Agullo-Rueda, E. E. Mendez, and J. M. Hong, Phys. Rev. B **40**, 1357 (1989).

[5] K. Fujiwara, H. Schneider, R. Cingolani, and K. Ploog, Solid State Commun. **72**, 935 (1989).

[6] J. Bleuse, G. Bastard, and P. Voisin, Phys. Rev. Lett. **60**, 220 (1988).

[7] E. Finkman, M. D. Sturge, and M. C. Tamargo, Appl. Phys. Lett. **49**, 1299 (1986).

[8] M. H. Meynadier, R. E. Nahory, J. M. Worlock, M. C. Tamargo, J. L. de Miguel, and M. D. Sturge, Phys. Rev. Lett. **60**, 1338 (1988).

[9] A. J. Shields, P. C. Klipstein, M. S. Skolnick, G. W. Smith, and C. R. Whitehouse, this issue, Phys. Rev. B **42**, 3599 (1990).

[10] D. M. Whittaker, Phys. Rev. B **41**, 3238 (1990).

[11] Details of the electronic properties of very similar structures grown in the same reactor are given in G. W. Smith, M. S. Skolnick, A. D. Pitt, I. L. Spain, C. R. Whitehouse, and D. C. Herbert, J. Vac. Sci. Technol. B **7**, 306 (1989).

[12] M. S. Skolnick, G. W. Smith, I. L. Spain, C. R. Whitehouse, D. C. Herbert, D. M. Whittaker, and L. J. Reed, Phys. Rev. B **39**, 11191 (1989).

[13] At zero electric field, the $\Gamma$-state Stokes shift, between the PL and PC (the feature labeled $g$) is $\sim 10$ meV for both structures. In finite fields, it is difficult to make any deductions about the magnitude of the shift since the PL transitions are unresolved, though for moderate fields they are probably dominated by the $\Gamma_{-1}$ transition as a result of thermalization (Ref. 1). The zero-field $\Gamma$ Stokes shift is larger than that observed for the $X$ states ($\sim 5$ meV), which is consistent with the greater importance of disorder-related effects, such as well-width fluctuations, for the ligher-mass $\Gamma$ electrons. The influence of well-width fluctuations is probably also the

reason for the greater width, compared to the $X$ peaks, of the $\Gamma$ transitions in both PL and PC, though an additional contribution due to lifetime broadening associated with the rapid relaxation to $X$ cannot be excluded [see Ref. 12 and J. Feldmann, R. Sattmann, E. O. Gobel, J. Kuhl, K. Ploog, R. Muralidharan, P. Dawson, and C. T. Foxon, Phys. Rev. Lett. **62**, 1892 (1989)].

[14]D. A. B. Miller, D. S. Chemla, T. C. Damen, A. C. Gossard, W. Wiegmann, T. H. Wood, and C. A. Burrus, Phys. Rev. B **32**, 1043 (1985).

[15]G. Bastard, Superlatt. Microstruct. **1**, 256 (1985).

[16]M. Altarelli, U. Ekenberg, and A. Fasolino, Phys. Rev. B **32**, 5138 (1988).

[17]B. Deveaud, A. Chomette, F. Clerot, A. Regreny, J. C. Maan, R. Romestain, G. Bastard, H. Chu, and Y. C. Chang, Phys. Rev. B **40**, 5802 (1989).

[18]R. H. Yan, R. J. Simes, H. Ribot, L. A. Coldren, and A. C. Gossard, Appl. Phys. Lett. **54**, 1549 (1989).

[19]D. Scalbert, J. Cernogora, C. Benoit à la Guillaume, H. Maaref, F. F. Charfi, and R. Planel, Solid State Commun. **70**, 945 (1989).

[20]In the present experiment, the photocreated-carrier density is sufficiently low that the excitons are well separated and only thermalization between states of a given exciton need be considered.